Theor Chim Acta (1992) 84: 125–133

Theoretica Chimica Acta

Heavy-atom tunneling in cyclobutadiene: *Ab initio* calculation of the intensities of a_g Raman lines*

P. Čársky[1] and J. Michl[2]

[1] J. Heyrovský Institute of Physical Chemistry and Electrochemistry, Czechoslovak Academy of Sciences, 18223 Prague 8, Czechoslovakia

[2] Department of Chemistry and Biochemistry, University of Colorado at Boulder, Boulder, CO 80309-0215, USA

Received June 25, 1992/Accepted July 8, 1992

Summary. GVB/[5*s*3*p*1*d*/3*s*1*p*] calculations were performed on the polarizability surface $\alpha(Я_1, Я_2, Я_3)$ of cyclobutadiene. The three a_g coordinates refer to automerization ($Я_1$), symmetric CC stretch ($Я_2$), and symmetric CCH bend ($Я_3$). This surface was used together with the previously obtained variational vibrational wave functions for the calculation of Raman intensities. The calculation predicts comparable intensities for the two split components of the automerization Raman line in an isolated molecule and disagrees with observations on matrix-isolated cyclobutadiene. The disagreement is attributed to the asymmetry of the double-well potential imposed by the effect of the Ar matrix.

Key words: Raman intensities – Tunneling – Cyclobutadiene – *Ab initio* calculations of polarizabilities – Variational calculation of vibrational levels

1 Introduction

The experimental data reported recently [1] for the Raman frequencies of cyclobutadiene (**1**) provided no evidence for the splitting of its a_g vibrational states predicted [2, 3] to result from heavy-atom tunneling. The experimental spectrum agrees better with that calculated in the harmonic approximation, in which the effects of tunneling are neglected altogether. However, Raman intensities had not been calculated and the interpretation was based on the first-order assumption that the +, + and −, − line pairs would appear with similar intensities. In principle, of course, the observation of a single peak for each transition might be due to a low intensity of one line in each such pair. We decided to verify the assumption by calculating the anharmonic Raman intensities of the split a_g lines.

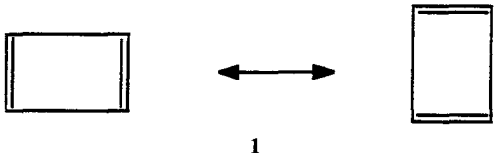

1

* Dedicated to Professor Ruedenberg

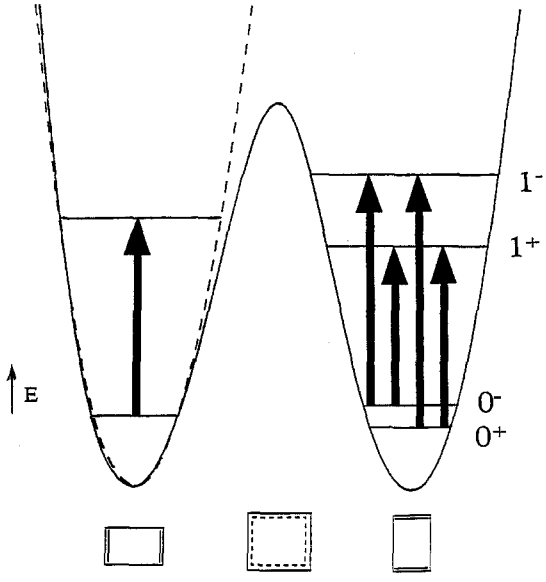

Fig. 1. Splitting of the cyclobutadiene a_g vibrational transitions in cyclobutadiene (schematic). Plotted horizontally is the automerization coordinate interconverting the two possible Kekulé structures. The dotted line in the left well represents the harmonic potential giving a single $0 \rightarrow 1$ transition for a_g modes. The effect of tunneling is shown in the right well. A splitting of the levels gives rise to four possible transitions for each a_g mode

The origin of the tunneling splitting is shown schematically in Fig. 1. The double-well character of the potential energy surface is due to the automerizing motion that interconverts the two possible Kekulé structures of cyclobutadiene (**1**). Although the barrier to automerization is rather high, about 10 kcal/mol [3–5], the potential well accommodates only three fairly strongly split automerization levels (0^+ and 0^-, 1^+ and 1^-, and 2^+ and 2^-). Vibrational levels for other modes are split indirectly, through their interaction with the automerization mode. Presently, we limit our attention to two other modes of the same a_g symmetry as the automerization, for which the coupling may be expected to be the strongest. These are the totally symmetric CC stretch and the totally symmetric CCH bend. As Fig. 1 shows, the tunneling splits each single line predicted by the harmonic approximation into four lines.

2 Calculations

2.1 Polarizability surface

As noted above and explained in detail in our earlier paper [2] it is convenient to reduce the problem of cyclobutadiene automerization to three dimensions and to use the following set of curvilinear symmetrized internal coordinates:

$$Я_1 = r_1 - r_2 \tag{1}$$

$$Я_2 = r_1 + r_2 - 2D \tag{2}$$

$$Я_3 = 8^{-1/2}(\beta_1 + \beta_2 + \beta_3 + \beta_4 - \beta_5 - \beta_6 - \beta_7 - \beta_8) \tag{3}$$

where r_1 and r_2 are the lengths of the CC bonds, D is the equilibrium CC bond length in the square structure, β_1, β_2, β_3 and β_4 are the valence angles between

the CH bonds and the longer CC bonds, and β_5, β_6, β_7 and β_8 are the valence angles between the CH bonds and the shorter CC bonds. The reference structure assumed, $Я_1 = 0$, $Я_2 = 0$ and $Я_3 = 0$, is the optimum square D_{4h} structure. To be consistent with our previous calculation of the potential energy surface [3], our task was to calculate the polarizability surfaces $\alpha_{xx}(Я_1, Я_2, Я_3)$, $\alpha_{yy}(Я_1, Я_2, Я_3)$ and $\alpha_{zz}(Я_1, Я_2, Я_3)$ in the GVB/[$5s3p1d/3s1p$] approximation. The α_{xy}, α_{xz}, and α_{yz} components vanish by symmetry. GVB was used because the square structure of cyclobutadiene is an open shell singlet and the simplest MO approach applicable to it is a two-configuration SCF-type method. The GVB polarizabilities were calculated analytically as second derivatives of energy with respect to the external electric field, using the formulas published by Yamaguchi et al. [6]. Although these authors were not the first to report analytical two-configuration SCF polarizabilities, their formulas seem to us more suitable for computer program coding than others available in the literature [7]. The [$5s3p1d/3s1p$] basis set was selected since it was especially tailored [8] to SCF calculations of polarizabilities. This basis set should yield a fairly accurate polarizability surface, since it is at least as good for this purpose as the 6-311++G(d, p) basis set, which gave excellent results [9] for the Raman intensities of benzene. We calculated 81 data points for different combinations of $Я_1$, $Я_2$, and $Я_3$.

For $-0.28 \leqslant Я_1 \leqslant 0.18$, we assumed the expansion:

$$\begin{aligned}\alpha_{xx} = {} & \alpha^0_{xx} + a_{1x} Я_1 + a_{2x} Я_1^2 + a_{3x} Я_1^3 + a_{4x} Я_1^4 + a_{5x} Я_1^5 \\ & + a_{6x} Я_1^6 + a_{7x} Я_1^7 + b_{1x} Я_2 + c_{1x} Я_1^2 Я_2 + d_{1x} Я_3 + d_{2x} Я_3^2 \\ & + e_{1x} Я_1 Я_3 + e_{2x} Я_1^2 Я_3 + e_{3x} Я_1 Я_3^2 \end{aligned} \tag{4}$$

and obtained the constants a_{ix} to e_{ix} by a least squares fit. Outside this range it was sufficient to fit α_{xx} by a simpler dependence on $Я_1$:

$$\begin{aligned}\alpha_{xx} = {} & \alpha_p + a_p Я_1 + b_{1x} Я_2 + c_{1x} Я_1^2 Я_2 + d_{1x} Я_3 + d_{2x} Я_3^2 + e_{1x} Я_1 Я_3 \\ & + e_{2x} Я_1^2 Я_3 + e_{3x} Я_1 Я_3^2 \quad \text{for } Я_1 < -0.28 \end{aligned} \tag{5}$$

$$\begin{aligned}\alpha_{xx} = {} & \alpha_q + a_q Я_1 + b_{1x} Я_2 + c_{1x} Я_1^2 Я_2 + d_{1x} Я_3 + d_{2x} Я_3^2 + e_{1x} Я_1 Я_3 \\ & + e_{2x} Я_1^2 Я_3 + e_{3x} Я_1 Я_3^2 \quad \text{for } Я_1 > 0.18 \end{aligned} \tag{6}$$

By symmetry,

$$\alpha_{yy}(Я_1, Я_2, Я_3) = \alpha_{xx}(-Я_1, Я_2, -Я_3) \tag{7}$$

Polarizability in the z direction (perpendicular to the molecular plane) could be fitted satisfactorily by a shorter expansion,

$$\alpha_{zz} = \alpha^0_{zz} + a_{1z} Я_1^2 + a_{2z} Я_1^4 + b_{1z} Я_2 + b_{2z} Я_2^2 + b_{3z} Я_1^2 Я_2 \tag{8}$$

for any value of $Я_1$. The optimum values of parameters in Eqs. (4–8) are summarized in Table 1.

2.2 Raman intensities

For the evaluation of Raman intensities we use the vibrational wave functions obtained previously [2, 3] by variational calculations, assuming a HBJ-type

Table 1. Optimized parameters for the GVB/[5s3p1d/3s1p] polarizability function[a]

$\alpha^0_{xx} = 6.556$ Å^3 [b]	$e_{2x} = 0.38779 \pm 0.16499$ Å
$a_{1x} = -8.9717 \pm 0.3389$ Å^2	$e_{3x} = 0.17367 \pm 0.03773$ Å^2
$a_{2x} = 11.346 \pm 1.309$ Å	$\alpha^0_{zz} = 4.813$ Å^3 [b]
$a_{3x} = 193.80 \pm 17.11$	$a_{1z} = -6.4518 \pm 0.0879$ Å
$a_{4x} = -164.22 \pm 27.39$ Å^{-1}	$a_{2z} = 13.802 \pm 0.640$ Å^{-1}
$a_{5x} = -1733.1 \pm 233.1$ Å^{-2}	$b_{1z} = 1.7930 \pm 0.0226$ Å^2
$a_{6x} = 621.97 \pm 127.72$ Å^{-3}	$b_{2z} = 0.26934 \pm 0.19594$ Å
$a_{7x} = 5295.8 \pm 882.7$ Å^{-4}	$b_{3z} = 3.5042 \pm 0.3762$
$b_{1x} = 2.7718 \pm 0.1839$ Å^2	$\alpha_p = 7.923$ Å^3
$c_{1x} = 8.0016 \pm 4.4983$	$a_p = 2.360$ Å^2
$d_{1x} = 0.51444 \pm 0.01439$ Å^3	$\alpha_q = 5.652$ Å^3
$d_{2x} = 0.12560 \pm 0.00883$ Å^3	$a_q = 1.897$ Å^2
$e_{1x} = -0.44459 \pm 0.03729$ Å^2	

[a] See Eqs. (4)–(8)

[b] This is the polarizability for the optimum square structure; the polarizability values for the optimum rectangular structure are: $\alpha_{xx} = 6.044$ Å^3, $\alpha_{yy} = 7.428$ Å^3, $\alpha_{zz} = 4.527$ Å^3 (the longer CC bond is along the x axis)

Hamiltonian [10]. These are in the form of products

$$\Psi_I = \sum_J C_{IJ} \Phi_{J,v_1}(S_1) \Phi_{J,v_2}(S_2) \Phi_{J,v_3}(S_3) \tag{9}$$

where the basis set functions $\Phi_{J,v_2}(S_2)$ and $\Phi_{J,v_3}(S_3)$ are the harmonic oscillator eigenfunctions and the functions $\Phi_{J,v_1}(S_1)$ were obtained in a pointwise form from a numerical solution of the one-dimensional Schrödinger equation for the automerization. S_1, S_2, and S_3 are linearized symmetry coordinates [2]:

$$\text{Я}_1 = S_1 - aS_3 \tag{10}$$

$$\text{Я}_2 = S_2 \tag{11}$$

$$\text{Я}_3 = S_3 + bS_2S_3 \tag{12}$$

where

$$a = R^0_{CH}\mu_C/(\mu_C + \mu_H) \tag{13}$$

$$b = 2^{-3/2}/(R^0_{CH}) \tag{14}$$

R^0_{CH} is the equilibrium CH bond distance and μ_C and μ_H are reciprocal atomic masses.

Substituting for the curvilinear coordinates in Eq. (4) and neglecting terms containing the fourth and higher powers of a, we obtain for $-0.28 \leqslant S_1 \leqslant 0.18$

$$\alpha_{xx} = \alpha^0_{xx} + \alpha_{xx}(S_1) + f_{2x}S_2 + f_{3x}S_3 + f_{33x}S_3^2 + f_{23x}S_2S_3 + f_{333x}S_3^3 + f_{233x}S_2S_3^2 + f_{2233x}S_2^2S_3^2 + f_{2333x}S_2S_3^3 + f_{22333x}S_2^2S_3^3 \tag{15}$$

$$\alpha_{yy}(S_1, S_2, S_3) = \alpha_{xx}(-S_1, S_2, -S_3) \tag{16}$$

where

$$\alpha_{xx}(S_1) = a_{1x}S_1 + a_{2x}S_1^2 + a_{3x}S_1^3 + a_{4x}S_1^4 + a_{5x}S_1^5 + a_{6x}S_1^6 + a_{7x}S_1^7 \tag{17}$$

$$f_{2x} = b_{1x} + c_{1x}S_1^2 \tag{18}$$

$$f_{3x} = d_{1x} - a(a_{1x} + 2a_{2x}S_1 + 3a_{3x}S_1^2 + 4a_{4x}S_1^3 + 5a_{5x}S_1^4 + 6a_{6x}S_1^5 + 7a_{7x}S_1^6) + e_{1x}S_1 + e_{2x}S_1^2 \tag{19}$$

$$f_{33x} = a^2(a_{2x} + 3a_{3x}S_1 + 6a_{4x}S_1^2 + 10a_{5x}S_1^3 + 15a_{6x}S_1^4 + 21a_{7x}S_1^5) + d_{2x} - ae_{1x} - 2ae_{2x}S_1 + e_{3x}S_1 \tag{20}$$

$$f_{23x} = bd_{1x} - 2ac_{1x}S_1 + be_{1x}S_1 + be_{2x}S_1^2 \tag{21}$$

$$f_{333x} = -a^3(a_{3x} + 4a_{4x}S_1 + 10a_{5x}S_1^2 + 20a_{6x}S_1^3 + 35a_{7x}S_1^4) - a^2e_{2x} - ae_{3x} \tag{22}$$

$$f_{233x} = a^2c_{1x} + 2bd_{2x} - abe_{1x} - 2abe_{2x}S_1 + 2be_{3x}S_1 \tag{23}$$

$$f_{2233x} = d_{2x}b^2 + e_{3x}b^2S_1 \tag{24}$$

$$f_{2333x} = -a^2be_{2x} - 2abe_{3x} \tag{25}$$

$$f_{22333x} = -ab^2e_{3x} \tag{26}$$

Outside this range of $\mathcal{R}_1$, Eqs. (5) and (6) yield

$$\alpha_{xx} = \alpha_p + a_pS_1 + f_{2x}S_2 + f_{3x,p}S_3 + f_{23x}S_2S_3 + f_{33x,p}S_3^2 + f_{333x,p}S_3^3 + f_{233x}S_2S_3^2 + f_{2233x}S_2^2S_3^2 + f_{2333x}S_2S_3^3 + f_{22333x}S_2^2S_3^3 \quad \text{for } \mathcal{R}_1 < -0.28 \tag{27}$$

$$a_{xx} = \alpha_q + a_qS_1 + f_{2x}S_2 + f_{3x,q}S_3 + f_{23x}S_2S_3 + f_{33x,q}S_3^2 + f_{333x,q}S_3^3 + f_{233x}S_2S_3^2 + f_{2233x}S_2^2S_3^2 + f_{2333x}S_2S_3^3 + f_{22333x}S_2^2S_3^3 \quad \text{for } \mathcal{R}_1 > 0.18 \tag{28}$$

where

$$f_{3x,p} = -a_pa + d_{1x} + e_{1x}S_1 + e_{2x}S_1^2 \tag{29}$$

$$f_{33x,p} = d_{2x} - ae_{1x} - 2ae_{2x}S_1 + e_{3x}S_1 \tag{30}$$

$$f_{333x,p} = -a^2e_{2x} - ae_{3x} \tag{31}$$

$$f_{3x,q} = -a_qa + d_{1x} + e_{1x}S_1 + e_{2x}S_1^2 \tag{32}$$

$$f_{33x,q} = f_{33x,p} \tag{33}$$

$$f_{333x,q} = f_{333x,p} \tag{34}$$

For the α_{zz} component we obtain

$$\alpha_{zz} = \alpha_{zz}^0 + \alpha_{zz}(S_1) + f_{2z}S_2 + f_{3z}S_3 + f_{22z}S_2^2 + f_{33z}S_3^2 + f_{333z}S_3^3 + f_{23z}S_2S_3 + f_{233z}S_2\,S_3^2 \tag{35}$$

where

$$\alpha_{zz}(S_1) = a_{1z}S_1^2 + a_{2z}S_1^4 \tag{36}$$

$$f_{2z} = b_{1z} + b_{3z}S_1^2 \tag{37}$$

$$f_{3z} = -2a_{1z}aS_1 - 4a_{2z}aS_1^3 \tag{38}$$

$$f_{22z} = b_{2z} \tag{39}$$

$$f_{33z} = a_{1z}a^2 + 6a_{2z}a^2S_1^2 \tag{40}$$

$$f_{23z} = -2b_{3z}aS_1 \tag{41}$$

$$f_{333z} = -4a_{2z}a^3S_1 \tag{42}$$

$$f_{233z} = b_{3z}a^2 \tag{43}$$

Now we are ready to evaluate the matrix elements

$$M_{\mu\mu}^{I,J} = \langle \Phi_{I,v_1}\Phi_{I,v_2}\Phi_{I,v_3}|\alpha_{\mu\mu}|\Phi_{J,v_1}\Phi_{J,v_2}\Phi_{J,v_3}\rangle, \tag{44}$$

$\mu = x, y, z$. The diagonal elements of the Raman scattering tensor

$$\alpha'_{\mu\mu}(KL) = \langle \Psi_L|\alpha_{\mu\mu}|\Psi_K\rangle \tag{45}$$

for the vibrational transition $K \rightarrow L$ are obtained as

$$\alpha'_{\mu\mu}(KL) = \sum_I \sum_J C_{KI}C_{LJ}M_{\mu\mu}^{I,J} \tag{46}$$

The mean value and anisotropy of α' were calculated as usual,

$$\alpha' = (1/3)(\alpha'_{xx} + \alpha'_{yy} + \alpha'_{zz}) \tag{47}$$

$$(\gamma')^2 = (1/2)[(\alpha'_{xx} - \alpha'_{yy})^2 + (\alpha'_{yy} - \alpha'_{zz})^2 + (\alpha'_{zz} - \alpha'_{xx})^2] \tag{48}$$

and the polarized Raman intensities were approximated by the following expressions:

$$I_\parallel = (\alpha')^2 + 4/45(\gamma')^2 \tag{49}$$

$$I_\perp = 1/15(\gamma')^2 \tag{50}$$

3 Results and comparison with experiment

The results of the calculations are summarized in Table 2. The calculated vibrational frequencies are overestimated, as is usual with SCF calculations, but if they are multiplied by the usual empirical factor of $\sqrt{0.8} = 0.89$, they agree well with the experimental a_g frequencies observed [1] at 992 (CCH bend), 1150 (CC stretch), and 1604 cm^{-1} (automerization). The splitting of the lines predicted for the CCH bend and CC stretch seems to be too small to be observable at the resolution available in the only experiment reported so far [1]. We therefore concentrate on the automerization transition, for which a large splitting is predicted. Since in the experiments of ref. [1] no polarizer was present in the path of the scattered light in order to maximize the observed intensity, and since the polarization bias of the analyzing grating monochromator is not known quantitatively, it is not clear that exact combination of $I_\parallel$ and $I_\perp$ should be used for the comparison. It is likely that $I_\parallel$ is the best choice.

Next we adjusted the Boltzmann populations of the 0^+00 and 0^-00 states by weighting the intensities by Boltzmann population factors $\exp(-E/kT)$ and by using the calculated energy difference, $E = 4.4$ cm^{-1}, between the 0^+00 and 0^-00 states. We evaluated the results at two temperatures that correspond to the temperature range in which spectra were measured [1] (4 and 25 K). At both temperatures the theory predicts two strong transitions of comparable intensity,

Table 2. Calculated Raman scattering tensor α' (Å^3) and Raman intensities (10^2 Å^6) for lowest-energy a_g transitions

Transition[a]	$\tilde{\nu}$ (cm^{-1})[b]	α'_{xx}	α'_{yy}	α'_{zz}	$I_\perp$	$I_\parallel$	$I_\parallel$ (4 K)[c]	$I_\parallel$ (25 K)[c]
$(0^+00)\rightarrow(0^+01)$	1162.3	−0.098	0.098	0.000	0.191	0.255	0.211	0.144
$(0^-00)\rightarrow(0^-01)$	1156.8	−0.094	0.094	0.000	0.177	0.236	0.040	0.103
$(0^+00)\rightarrow(0^-01)$	1161.2	0.008	0.008	−0.006	0.001	0.003	0.003	0.002
$(0^-00)\rightarrow(0^+01)$	1157.9	−0.001	−0.001	−0.004	0.000	0.000	0.000	0.000
$(0^+00)\rightarrow(0^+10)$	1304.0	0.131	0.131	0.008	0.100	0.939	0.779	0.529
$(0^-00)\rightarrow(0^-10)$	1318.4	0.132	0.132	0.014	0.092	0.975	0.166	0.426
$(0^+00)\rightarrow(0^-10)$	1322.8	−0.041	0.041	0.000	0.033	0.044	0.036	0.025
$(0^-00)\rightarrow(0^+10)$	1299.6	−0.025	0.025	0.000	0.013	0.017	0.003	0.007
$(0^+00)\rightarrow(1^+00)$	1920.3	−0.053	−0.053	−0.130	0.039	0.677	0.562	0.381
$(0^-00)\rightarrow(1^-00)$	1986.6	−0.052	−0.052	−0.132	0.042	0.673	0.115	0.294
$(0^+00)\rightarrow(1^-00)$	1991.0	−0.063	0.063	0.000	0.080	0.107	0.089	0.060
$(0^-00)\rightarrow(1^+00)$	1915.9	−0.039	0.039	0.000	0.031	0.041	0.007	0.018

[a] The transitions are characterized by the basis set functions Φ with the largest weights; the quantum numbers are in the order automerization, CC stretch and CCH bend; the transitions are grouped in quadruplets and ordered in the sequence $++$, $--$, $+-$, and $-+$ (Fig. 1)

[b] Unscaled GVB/[5*s*3*p*1*d*/3*s*1*p*] frequencies from ref. [3]

[c] Boltzmann-weighted intensities

split by 66 cm^{-1}, and two very weak transitions, as expected from first-order theory. This disagrees with the experiment, in which only a single band was observed in the automerization region.

Clearly, this disagreement can no longer be rationalized by postulating a much weaker intensity for one of the Raman lines, unless one wishes to claim that we have used an insufficiently accurate potential function, or oversimplified electronic wave functions, and this strikes us as unlikely. It seems much more probable that the origin of the disagreement lies in the sensitivity of the Raman spectrum to matrix-imposed asymmetry of the double-well potential. Leclercq and Sandorfy [11] examined the effect of the symmetry reduction on resonance Raman intensity. Calculations by Kofranek et al. [12] on the effect of the Ar matrix on the structure of cis-butadiene suggest that the energy difference between two rectangular forms of cyclobutadiene in the Ar matrix may be as high as 1 kcal/mol.

We tried to simulate the effect of asymmetry by adding a linear term, $K_{as}\mathcal{R}_1$, to the potential function $V(\mathcal{R}_1, \mathcal{R}_2, \mathcal{R}_3)$. The constant K_{as} was adjusted so as to give at most $\Delta E = 1$ kcal/mol (in which case it is 0.0158 mdyne) for the energy difference between the two potential wells. The asymmetry in the well depths can be expected to cause a mixing of the "plus" and the "minus" vibrational wave functions, and a localization of the resulting functions in one or the other well. It should have two important spectral effects. First, the magnitude of the splitting between the two predicted strong automerization lines will change. Second, the lower-energy well becomes more strongly populated than the other well, and the intensities of the two predicted lines will change correspondingly. The calculated effect of ΔE on the splitting between the strong automerization lines is plotted in Fig. 2. The splitting of 66 cm^{-1} predicted for the symmetric double-well potential is seen to drop rapidly as a small asymmetry is imposed. It becomes zero when ΔE reaches a value of about 0.5 kcal/mol. For larger ΔE values, the lines exchange their positions and the splitting grows again.

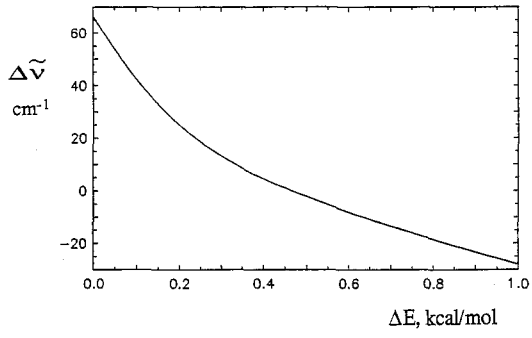

Fig. 2. Splitting of the automerization line (in cm^{-1}) as a function of the imposed asymmetry in the potential. ΔE is the energy difference between the bottoms of the two potential wells

Even for ΔE as small as 0.1 kcal/mol, the upper-well ground state lies 35 cm^{-1} above the lower-well ground state and its population at 25 K is only 12%. Although the calculated intrinsic intensities $I_{\|}$ for the automerization transitions from these states are close in absolute value, 0.00546 and 0.00566 $Å^6$, the latter is predicted to be about 10 times weaker than the former because of the different populations of the ground states in the two wells: the Boltzmann-weighted intensities $I_{\|}$ are 0.00482 and 0.00067 $Å^6$. For larger values of ΔE, the intensity difference is even larger, but already the miniscule matrix-induced energy difference of 0.1 kcal/mol between the two rectangular forms would be clearly sufficient for a rationalization of the experimental observation of a single line (Fig. 3). We

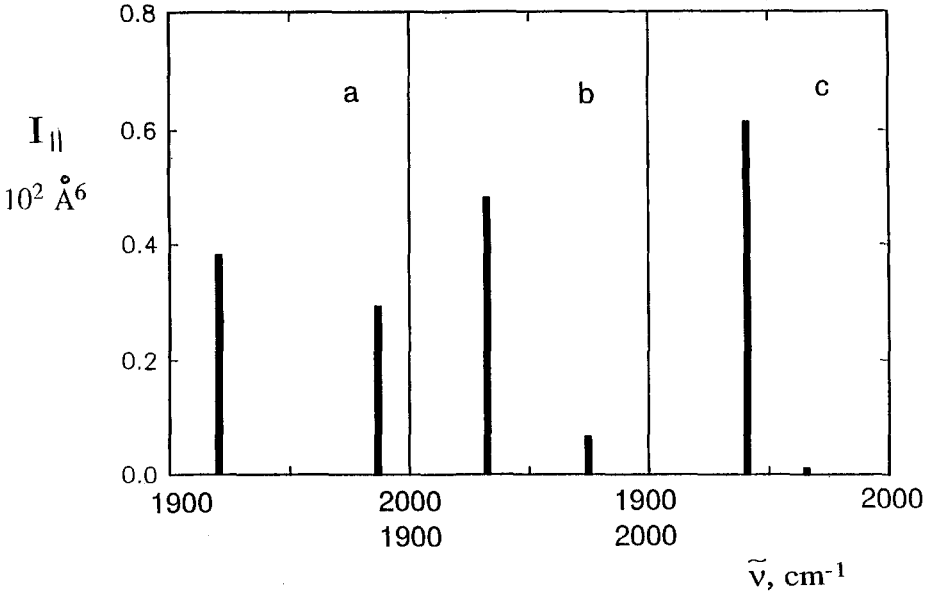

Fig. 3. Calculated splitting and Boltzmann-weighted intensities $I_{\|}$ of the automerization transitions $(0^+00) \rightarrow (1^+00)$ and $(0^-00) \rightarrow (1^-00)$ at 25 K as a function of the imposed asymmetry ΔE (see Fig. 2). The frequencies are the unscaled GVB/[5*s*3*p*1*d*/3*s*1*p*] frequencies from ref. [3]. **a** $\Delta E = 0$; **b** $\Delta E = 0.1$ kcal/mol; **c** $\Delta E = 0.2$ kcal/mol

conclude that it will be very difficult to obtain frequency-domain Raman spectroscopic evidence for heavy-atom tunneling in cyclobutadiene (**1**) unless the environment has a four-fold symmetry and does not remove the degeneracy of the two Kekulé structures.

Acknowledgement. This project was supported by the National Science Foundation (CHE 9000292 and CHE 9022151).

References

1. Arnold BR, Radziszewski JG, Campion A, Perry SS, Michl J (1991) J Amer Chem Soc 113: 692
2. Čársky P, Špirko V, Hess BA Jr, Schaad LJ (1990) J Chem Phys 92:6069
3. Čársky P, Downing JW, Michl J (1991) Int J Quantum Chem 40:415
4. Arnold BR, Michl J (1990) Spectroscopy of cyclobutadiene. In: Platz MS (ed) Kinetics and spectroscopy of carbenes and biradicals. Plenum, NY, p 1–35
5. Maier G (1988) Angew Chem Internat Ed Engl 27:309
6. Yamaguchi Y, Frisch MJ, Lee TJ, Schaefer HF III, Binkley JS (1986) Theor Chim Acta 69: 337
7. For references see Jørgensen P, Simons J (eds) (1986) Geometrical derivatives of energy surfaces and molecular properties. Reidel, Dordrecht, The Netherlands
8. Sadlej J (1988) Collect Czech Chem Commun 53:1995
9. Ozkabak AG, Thakur SN, Goodman L (1991) Int J Quantum Chem 39:411
10. Hougen JT, Bunker PR, Johns JWS (1970) J Mol Spectrosc 34:136
11. Leclercq JM, Sandorfy C (1983) J Raman Spectrosc 14:358
12. Kofranek M, Karpfen A, Lischka H (1992) Chem Phys Lett (in press)